Formation of Acetylcholine Receptor Clusters in Chick Myotubes: Migration or New Insertion?

Janet M. Dubinsky,* David J. Loftus,‡ Gerald D. Fischbach,* and Elliot L. Elson‡

*Department of Anatomy and Neurobiology, and ‡Department of Biochemistry, Washington University School of Medicine, St. Louis, Missouri 63110

Abstract. Experiments were performed to study the feasibility of two mechanisms of acetylcholine receptor (ACHR) accumulation in chick myotubes: diffusion and trapping of previously dispersed surface receptors and localized insertion of new receptors at accumulation sites. Fluorescence photobleaching recovery (FPR) measurements indicated that the majority of diffusely distributed ACHRs in chick myotube membranes were mobile whereas nearly all receptors within high density clusters were effectively immobile. Unlike previous reports, two rates of ACHR movement characterized the mobile population. Moreover, we found that the estimated diffusion coefficient depended critically on the objective (spot size) used to assay recovery from bleaching. Implications of this finding for mechanisms of receptor immobilization are discussed. Extracts of chick brain, known to increase the number of surface receptors, did not alter receptor mobility. Extracts of Torpedo electric organ that increase the number of receptor aggregates, decreased the mobile fraction of ACHRs. Simulations of the diffusion and trapping mechanism indicated that captured receptors should congregate around the periphery of a receptor patch during the first hour after they were inserted into the membrane. However, newly inserted ACHRs were found to be located centrally within receptor patches under neurites, and this was not consistent with an exclusive diffusion-trapping mechanism. We also studied the mobility of ACHRs near points of contact made by cholinergic growth cones. The rate of receptor movement was increased in the vicinity of growth cones, but the magnitude of this effect was small.

IN uninnervated cultured myotube membrane, acetylcholine receptors (ACHRs)[1] are both diffusely distributed over the surface and concentrated in aggregations termed hot spots. (The terms receptor patch, cluster, aggregation, or accumulation refer to a surface area containing a high density of ACHRs in either uninnervated (hot spots) or innervated (NARPs) myotubes.) When a neurite grows over a myotube, existing receptor accumulations disperse and new aggregations are formed under the neurite (Anderson and Cohen, 1977; Frank and Fischbach, 1979; Kuromi and Kidokoro, 1984). These neurite-associated receptor patches (NARPs) may form as a result of local insertion of newly synthesized ACHRs at appropriate sites (Stya and Axelrod, 1983; Role et al., 1985). Indeed, the neurite may secrete a substance that controls the rate of ACHR synthesis and insertion (Buc-Caron et al., 1983; Usdin and Fischbach, 1986; Harris et al., 1988). In cultured chick myotubes, newly inserted ACHRs account for 60–80% of all receptors at developing NARPs

A brief account of this work has appeared in abstract form (1987. *Soc. Neurosci. Abstr.* 13:373. [Abstr.]).

1. *Abbreviations used in this paper:* ACHR, acetylcholine receptor; BTX, α-bungarotoxin; CBE, chick brain extract; FPR, fluorescence photobleaching recovery; NARP, neurite-associated receptor patch; RBTX, rhodaminated-α-bungarotoxin; TEOE, Torpedo electric organ extract.

(Role et al., 1985). Alternatively, NARP formation may occur principally from the migration of exposed surface receptors to the site of nerve–muscle contact (Edwards and Frisch, 1976; Anderson and Cohen, 1977; Kuromi et al., 1985). Previously, estimates of ACHR mobility made with fluorescence photobleaching recovery (FPR) yielded widely divergent values. In rat myotubes, ACHR diffusion coefficient ranges from 5×10^{-11} cm²/s (Axelrod et al., 1976) to 1×10^{-10} cm²/s (Stya and Axelrod, 1984). In *Xenopus* myocytes FPR measurements produced an ACHR diffusion coefficient of 2.5×10^{-10} cm²/s Kuromi et al., 1985), while an iontophoretic technique yielded a value of 2.6×10^{-9} cm²/s (Poo, 1982). Few data are available on the chick system (Axelrod et al., 1978) in which insertion has been studied extensively (Devreotes et al., 1977; Usdin and Fischbach, 1986; Role et al., 1985).

In this paper, the mechanisms contributing to receptor patch formation in chick myotubes were explored using FPR measurements of the mobility of ACHRs in uninnervated myotubes. The chick system is ideal for these studies since in both mature, embryonic, and cultured muscle, the neuromuscular junction is not invaginated (Hirano, 1967; James and Tresman, 1969; Cohen and Pumplin, 1979; Burrage and Lentz, 1981) and movements of ACHRs can be studied in the

plane of the myotube surface. Extreme care was taken to fully characterize the mobile behavior of chick ACHRs. The observed rates of movement were consistent with the migration and trapping mechanism. The effects of cholinergic growth cones and two factors that modify ACHR accumulation upon the measured rates of ACHR mobility were evaluated. Newly inserted receptors, which constitute the majority of ACHRs at forming NARPs, were examined using fluorescence microscopy. Combining the measurements of ACHR mobility with observed patterns of ACHRs at developing NARPs, the behavior of newly inserted receptors was modeled. Our results were more consistent with localized insertion of ACHRs into NARPs than with accumulation of dispersed receptors by diffusion and trapping.

Materials and Methods

Cell Culture

Cultures of chick pectoral myotubes were grown on glass cover slips or glass bottomed petri dishes according to established procedures (Fischbach, 1972; Role et al., 1985) in MEM containing 10% horse serum, 0.29 μg/ml glutamine, 50 U/ml penicillin and 50 μg/ml streptomycin and 5% chick embryo extract. For the factor experiments, cells were grown in similar MEM with 40 mg/ml conalbumin substituted for the embryo extract. 3 d after plating the medium was changed to include 10^{-5} M cytosine arabinoside. In some experiments, dissociated ciliary neurons were added to myotube cultures on day 4 (Nishi and Berg, 1977; Role et al., 1985). All cultures were incubated with rhodaminated-α-bungarotoxin (RBTX; $\sim$15 nM) for 1 h before viewing (Ravdin and Axelrod, 1977). Cells were placed in a Hepes-buffered physiological salt solution for photobleaching experiments.

Fluorescence Photobleaching Recovery Measurements

For most experiments, a 40× 0.75 NA water immersion objective (Carl Zeiss, Inc., Thornwood, NY; beam radius, w = 2.06 μm) was used. In some experiments, an 100× 1.30 NA oil immersion neofluar (Carl Zeiss, Inc.; w = 0.84 μm) or a 16× 0.35 NA plan objective (Carl Zeiss, Inc., w = 4.14 μm) was used. The e^{-2} beam radius (w) was calibrated by fitting a theoretical Gaussian profile to a digital image of the emission from a thin-layer sample of rhodamine B dried onto a microscope slide illuminated with the monitor beam. The standard deviation of the beam radius calibrations was <6%. The image processing system used consisted of a camera (model 68, ISIT; Dage-MTI Inc., Wabash, MI), image processor (model CMR 270; Control-3M Image Processing Systems, Pasadena, CA), and a computer (MicroVax II; Digital Equipment Corp., Maynard, MA).

Photobleaching was accomplished by a brief pulse of intense laser illumination. Light energy incident upon the myotube surface was determined from the calibrated light output of the laser and the calibrated light losses through the optical system. Bleach energy per unit area was held constant for the different objectives at 700 W-s/cm² by shortening the bleach time for the smaller beam radii. This allowed the minimum possible bleach duration to be used for each objective (5 ms for the 40×), while maintaining uniform bleach depth (50–75%). In a few experiments that were done using higher and lower bleach energy, however, the diffusion coefficient and mobile fraction were not found to be dependent on bleach depth (data not shown).

For the 40× objective, fluorescence recovery was monitored continuously for 75 s with a monitor beam intensity of 15 W/cm². When recovery was measured for 750 s, an intensity of 0.3 W/cm² was used. Control experiments showed that intermittent monitoring of fluorescence recovery gave the same results as continuous monitoring (data not shown). For the 16× objective, fluorescence recovery was monitored intermittently over 300 s with an effective intensity of $\sim$3 W/cm². For the 100× objective, continuous recovery was monitored for 75 s with a monitor beam intensity of 15 W/cm². To improve the signal to noise ratio for the 100× objective, 3–5 recovery curves from different spots on each myotube were added together before analysis. For all experiments, monitor phase bleaching, defined as fluorescence decline in the absence of a high intensity bleaching pulse, was <10%.

FPR Analysis

Fluorescence recovery traces were analyzed individually and fit to a single recovery phase (Axelrod et al., 1976; Koppel et al., 1976), from which the characteristic diffusion time t_d and the mobile fraction X_m were calculated. Analysis of variation demonstrated no significant difference in these parameters from cell to cell, culture dish to culture dish, or day to day. Hence all of the data were averaged. From the average value of t_d, the diffusion coefficient D was calculated from $D = w^2/4t_d$ (Koppel et al., 1976). The SEM for D (DD) was calculated from $DD = (Dt_d/t_d) \cdot D$, where Dt_d is the SEM for t_d.

Long time scale experiments (40× objective, 750-s recovery) exhibited two mobile phases, corresponding to the fast phase measured above and an additional slow phase. For each long time scale measurement, short time scale (fast phase) data was obtained from a nearby region on the same myotube. Analysis of the slow phase of recovery was accomplished by (a) normalizing the prebleach intensities; (b) subtracting the fast phase data from long time scale data, and then (c) fitting the remaining slow phase as a single phase of recovery. Since the subtraction procedure introduced some additional noise, the data from seven different myotubes were summed (yielding a single curve) before fitting. Statistics for the mobile fraction and diffusion coefficient of the slow phase, therefore, could not be calculated.

Diffusion-trapping Model

The mobile behavior of newly inserted ACHRs was modeled for a 512 × 512 pixel array with a Fortran program run on a computer (MicroVax II; DEC). Individual steps of one pixel corresponded to a 0.125-μm displacement and occurred every 61 ms, equivalent to a diffusion coefficient of 6.4 × 10^{-10} cm²/s (see Results). At each time increment, a receptor was permitted to move one pixel, up, down, or sideways but not diagonally, as determined by a call to a pseudo-random number generator. Cycling of the pseudo-random number generator was prevented by periodically restarting it with a randomly selected seed. New receptors were added at randomly chosen pixels with a probability of appearance of 3.6 receptors/μm/h (Falls and Fischbach, personal communication) or 0.213 receptors/time increment. Only 40% of these receptors (representing the fast phase) were permitted to move. When a receptor entered a trap area either by migration or direct insertion, its motion was limited by an additional probability (p = 0.052) factor that slowed its diffusional rate to the maximum value estimated for receptors within aggregates, 3.3 × 10^{-12} cm²/s (see Results). Receptors were permitted to leave the trap if so directed. Thus, the apparent trap efficiency depended upon the contour of the perimeter and varies with time as trapped receptors move towards the interior. Anchor or immobilization sites were defined as all pixels above an arbitrary intensity in fluorescence video images of NARPs. Receptors were allowed to leave the trapped areas. Multiple receptors were allowed to occupy the same pixel, but their subsequent motions were calculated independently.

Measurement of Newly Inserted Acetylcholine Receptors

Unlabeled α-bungarotoxin (BTX) was added to cocultures at the time of neuronal plating. 15 h later, BTX was removed and 0 or 6 h elapsed before a subsequent 1-h incubation with RBTX and mAb 35, an mAb directed against the alpha subunit of the ACHR (Tzartos et al., 1981). mAb 35 labeling was visualized using goat anti-rat FITC-IgG (Organon Teknika-Cappel, Malvern, PA). After fixation in 4% paraformaldehyde, these dishes were viewed on a microscope with a 100× 1.3 NA oil objective (E. Leitz, Rockleigh, NJ). Fixation of cultures before mAb 35 labeling did not alter the appearance of receptor clusters. In control experiments in which unfixed, live myotubes labeled with mAb 35 were directly observed, antibody-induced receptor aggregation and internalization did not occur until 3–5 h after completion of the mAb 35 and secondary antibody incubations. Therefore, binding of mAb 35 and secondary antibody to receptors did not alter their distribution in the membrane.

NARPs were located in phase-contrast and the associated fluorescein (excite, 450–490 nm and emission bandpass, 515–530 nm) and rhodamine (excite, 530–560 nm and emission bandpass >580 nm) emissions were captured with a camera (model 66, SIT; Dage-MTI Inc.) on automatic settings and digitized and analyzed with an image processor (5500 series, Trapix; Recognition Concepts, Inc., Incline Village, NV) connected to a computer (MicroVax II; DEC).

Factor Preparation

Partially purified chick brain extract (CBE) was prepared according to Usdin and Fischbach (1986) by Dr. Douglas Falls. Briefly, acid extracts of chick brain were chromatographed on CM-Sephadex. Active fractions were loaded onto a semipreparative Vydac C4 column that was eluted with isopropyl alcohol in trifluoroacetic acid. Aliquots of those fractions that contained biological activity (increased the rate of incorporation of chick ACHRs) were used. These are the initial purification steps in the preparation of a protein called ARIA (Usdin and Fischbach, 1986). Torpedo electric organ extracts (TEOE) were partially purified from insoluble fractions of Torpedo electric organ basement membrane by a pH 5.5 citrate extraction (Godfrey et al., 1984) by Dr. Leland Scott. Further purification of this extract yields a factor called AGRIN (Godfrey et al., 1984; Nitkin et al., 1987). In separate tests, Torpedo electric organ extract increased greater than threefold the number of ACHR patches on the bottom surface of chick myotubes in vitro. On day 4 (TEOE) or days 6 or 7 (CBE), myotubes were fed with medium supplemented with an aliquot of one of the partially purified factors. 24 h later, cells were rinsed and incubated with RBTX in MEM for 1 h before FPR measurements.

Results

Mobility of ACHRs

ACHR mobility was measured by monitoring FPR of RBTX-labeled myotubes (Fig. 1, Table I). As expected, no appreciable recovery of fluorescence was observed in hot spots on uninnervated myotubes (Fig. 1 A) or in neurite-associated receptor patches (NARPs) in nerve–muscle cocultures. In some instances, where the receptor patch did not entirely fill the laser spot ($w = 2.06$ μm; 40× objective, 75-s recovery time), the small amount of recovery (<10%) was attributable to the adjacent diffuse areas. For large hot spots (>4 μm diameter) in which recovery was monitored for 12.5 min, a maximum of 5.1% recovery was measured. Receptors within hot spots were thus effectively immobile, with an upper limit for their diffusion coefficient of 3.3 × 10^{-12} cm^2/s (t_d = 3 h). These results are similar to those estimated for rat myotubes and *Xenopus* myocytes (Axelrod et al., 1976; Kuromi and Kidokoro, 1984; Kuromi et al., 1985).

Specific RBTX label was detectable in areas of myotube membrane devoid of ACHR patches. Fluorescence associated with ACHR patches was absent and extra-cluster fluorescence was not detectable by eye when myotubes were exposed to a 100-fold excess of unconjugated BTX in the presence of RBTX. Myotube autofluorescence in the absence of label and nonspecific label associated with the substrate and with fibroblasts in the cultures amounted to <10% (average 4%) of diffuse area photometer counts.

In contrast to the situation observed at clusters, after diffuse areas of both innervated and uninnervated myotubes were bleached, fluorescence gradually recovered to ∼40% of the initial value in 75 s (Fig. 1 B). Calculations based on this rate of recovery indicated that 43 ± 3% ($N = 114$, 40× objective) of RBTX-labeled ACHRs were mobile with a diffusion coefficient of $D = 6.4$ × 10^{-10} cm^2/s. We also measured fluorescence recovery on a longer time scale, up to 12.5 min. As shown in Fig. 1 C, two phases of recovery were observed. After the initial fast phase of recovery, an additional 31% of the fluorescence intensity recovered at a slower rate. We estimate the diffusion coefficient of the slow phase to be $D = 3.3$ × 10^{-11} cm^2/s. Considering both the fast phase and the slow phase, a total of 74% of ACHRs were mobile. However, since a small amount of "monitor phase
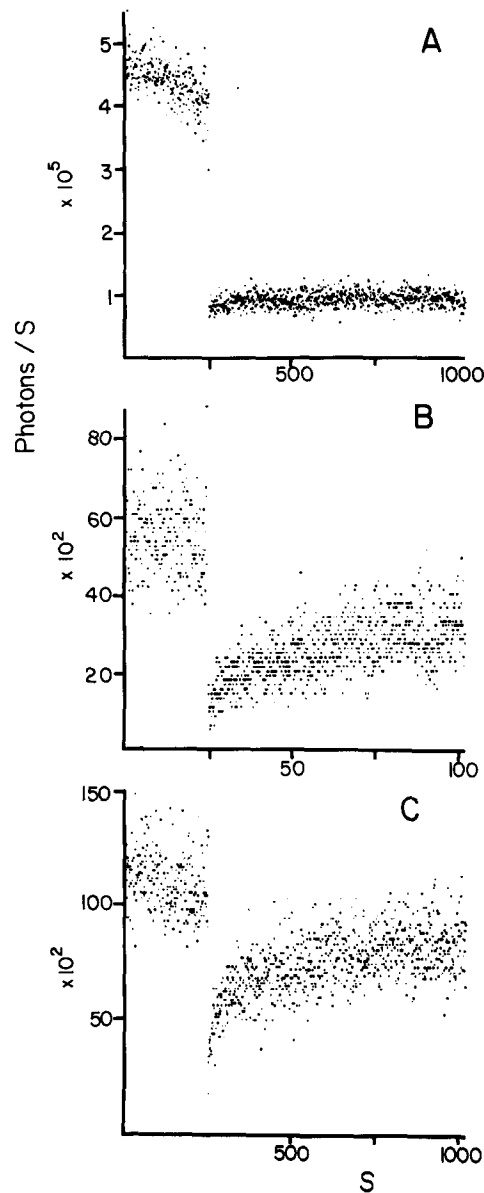

Figure 1. FPR of RBTX labeled ACHRs on myotube membranes. (*A*) Long time scale measurement of ACHR mobility in receptor patches. Up to 12.5 min after the bleach, no more than 5.1% mobility was detected. (*B*) Short time scale measurement in diffuse areas, using a 40× objective. A mobile fraction $X_m = 43\%$ was measured, with an apparent diffusion coefficient $D = 6.4 \times 10^{-10}$ cm^2/s. (*C*) Long time scale measurement in diffuse areas, using a 40× objective, exhibits a second mobile phase with an apparent diffusion coefficient $D = 3.3 \times 10^{-10}$ cm^2/s, which contributes an additional 31% recovery.

bleaching" (gradual bleaching while monitoring recovery) could not be eliminated in these long time scale experiments, we considered 74% to be a lower limit for the total mobility. It is possible that 100% of ACHRs were mobile in diffuse areas. This is the first observation that ACHRs move at two distinct rates in the myotube membrane.

Additionally, decreasing the monitor phase intensity over a fourfold range did not alter the two phase diffusion process. Therefore, it is unlikly that intensity (e.g., photochemical

Table I. ACHR Diffusion Coefficients and Mobile Fractions in Diffuse Areas and in Receptor Patches, as Measured with a 40× Objective (w, 2.06 μm)

Region	X_m (SEM)	D (SEM)	N
	%	cm^2/s	
Diffuse areas (Fast phase)	43* (3)	6.4×10^{-10} (0.7×10^{-10})	114
Diffuse areas (Slow phase)	31* (‡)	3.3×10^{-11}	7
Hot spots and NARPS	4.9§ (0.8)	$<3.3 \times 10^{-12}$	56

* Total fractional recovery calculated from fitted recovery curve.
‡ Seven traces were combined before fitting (see Materials and Methods).
§ Fractional recovery measured 75 s after bleach.

Table II. Mobile Fractions, Characteristic Recovery Times, and Apparent Diffusion Coefficients for the Fast Phase of ACHRs as Measured with Different Objectives

Objective	Beam radius, w	X_m	t_d	$D_{Apparent}$
	μm	%	s	cm^2/s
100×	0.84	38	13.2	1.3×10^{-10}
40×	2.06	43	16.7	6.4×10^{-10}
16×	4.14	41	55.2	7.8×10^{-10}

effects) can account for the two mobile phases that were observed.

The fast phase diffusion coefficient we have measured ($D = 6.4 \times 10^{-10}$ cm²/s) was severalfold faster than the value of $D = 1 \times 10^{-10}$ cm²/s interpolated from Fig. 2 of Axelrod et al. (1978) for the diffusion coefficient of ACHRs on chick myotubes. An important difference in experimental method between our results and those of Axelrod et al. might be that we used a 40× objective (beam radius $w = 2.06$ μm), whereas Axelrod and co-workers used a 100× objective (beam radius $w = 0.9$ μm). Therefore, to obtain directly comparable data, we examined the mobility of the fast phase of mobile ACHRs using different objectives.

Surprisingly, we found that the apparent fast phase diffusion coefficient for ACHRs in diffuse areas was dependent on the beam size (Fig. 2; Table II). In particular, when FPR measurements were made with a 100× objective, the measured characteristic diffusion time (t_d) of 13.2 s was about fivefold higher than the value of 2.7 s predicted from the calibrated beam radius and the results for the 40× objective (Fig. 2 A). Thus, the apparent fast phase diffusion coefficient for ACHRs was only $D = 1.3 \times 10^{-10}$ cm²/s, approximately fivefold lower than the result obtained with the 40× objective
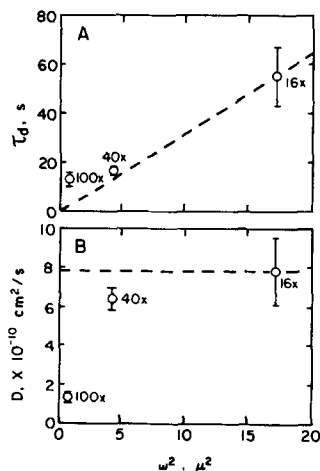

Figure 2. (A) The apparent recovery time t_d as a function of w^2, as determined in FPR experiments examining the fast phase of mobile ACHRs in diffuse areas. The dashed line indicates the expected relationship based upon the fastest apparent diffusion coefficient measured with the 16× objective. (B) The apparent diffusion coefficient as a function of w^2 calculated from the measured recovery times (t_ds) above. The apparent diffusion coefficient for the 100× objective is six times lower than the apparent diffusion coefficient for the 16× objective.

(Fig. 2 B). The mobile fraction for the 100× objective data was 35% (comparable to that measured with the 40× objective) indicating that only the fast phase of mobile ACHRs was being measured and the value for the diffusion coefficient was not "contaminated" by recovery of the slow mobile phase of ACHRs. In contrast, FPR experiments with the 16× objective yielded comparable results to the 40× objective (Table II). Between $w = 2.06$ μm and $w = 4.14$ μm, t_d scaled directly with w^2. For the 100× objective, the characteristic diffusion time, t_d, did not scale with w^2, as predicted by a model for simple diffusion: $t_d = w^2/4D$.

Hence, we have observed that dispersed receptors exist in at least two mobility classes with diffusion coefficients near (6.4 and 0.33) × 10^{-10} cm²/s. In addition, the mechanism of the fast phase of diffusion appeared complex. The discrepancy between apparent diffusion coefficients measured with the 100× and 40× objectives implied that more than one physical process was involved (see Discussion).

Diffusion-trapping Model of Newly Inserted Receptors

Both of these diffusion rates were in a range where capture of mobile ACHRs could conceivably contribute substantially to receptor patch formation (Strollberg and Fraser, 1988). To test the feasibility of this mechanism, we modeled the motion of newly inserted ACHRs in a 1,110 μm² section of myotube membrane that included a NARP as a trap. The model embodied the most conservative values. Hence, of the diffuse receptors, only those moving in the fast phase were considered and the trapping was not 100% efficient. Although the measured diffusion coefficients were based on all receptors, newly inserted molecules were assumed to behave in the same manner as preexisting ones. 70 min of real time were simulated as described in Materials and Methods.

Results for two NARPs are shown in Fig. 3. Those receptors trapped in the anchored areas clearly formed an annular pattern around the periphery. Migration within anchored areas filled small NARPs (arrows) but receptors did not significantly extend into larger NARPs (arrowheads). The groups of small receptor aggregates appeared to hinder the paths for freely diffusing particles so that few receptors accumulated within the center of the composite NARP. Similar patterns were produced even when the rate of insertion of new receptors was increased to 20 receptors/μm²/h. If the slowly diffusing receptors were added to the model and the receptors were not allowed to leave the trap, the annular pattern would predictably be enhanced.

Visualization of Newly Inserted ACHRs

Newly inserted ACHRs were measured to determine if they conformed to the predicted annular patterns. Newly inserted
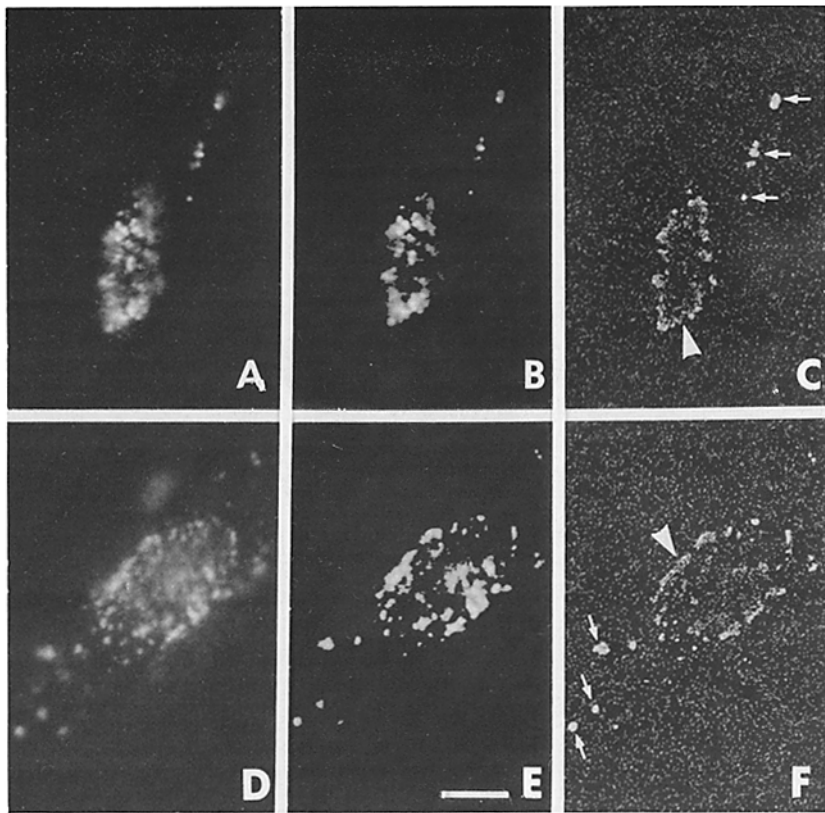
Figure 3. Two examples of computer modeling of diffusion and trapping of newly inserted ACHRs. A and D are fluorescein images of mAb 35 postlabeled NARPs prepared as described in Materials and Methods. B and E show the pixels selected to act as a template for the trap. C and F present the simulated 70 min of migration and trapping. Each individual ACHR is represented by the lowest intensity dot visible. Accumulations of more than one receptor per pixel are proportionately more intense. Arrows indicate small NARPs completely filled in with new receptors. ACHRs accumulate within larger NARPs in an annular pattern (arrowheads). Only a portion of the 33-μm $\times$ 33-μm modeled field is shown. Bar, 10 μm.

ACHRs were visualized with RBTX after previous block of all exposed receptors with unconjugated BTX as described in Materials and Methods. Both new and old receptors were labeled with mAb 35 and a fluoresceinated secondary antibody. These measurements were made in neuron–myotube cocultures 15 h after plating the neurons, when the contribution of newly inserted receptors to developing NARPs is maximal (Role et al., 1985). Newly inserted receptors within hotspots were not studied since their time of origin was unknown.

Seven hours after cold block, new ACHRs labeled with RBTX precisely colocalized with mAb 35 signal (data not shown). To determine if new receptors were preferentially inserted in these spots, clusters were examined only 1 h after removal of block of exposed sites. The rate of insertion of ACHRs at developing NARPs was indeed high enough that the newly inserted receptors could be visualized in such a short time. In many instances, the pattern of newly inserted receptors was strikingly similar to the pattern of all receptors (Fig. 4). Portions of the NARP where the mAb 35 immunoreactivity was more intense corresponded to portions where the RBTX signal was more intense. This implies that the rate of insertion is proportional to the density of existing ACHRs. However, not all areas of every NARP received equal amounts of new ACHRs. Two small clusters (Fig. 4 B, arrows) had no corresponding new receptors, while areas of comparable density in the large NARP had varying amounts of new insertion. New receptors typically appeared punctate or clustered. Significantly, no annuli or staining along the outer rims of NARPs were detected in the 73 NARPs examined. The measured patterns of newly inserted receptors did

not correspond to the patterns predicted by the diffusion-trapping mechanism (compare Fig. 4, D and H with Fig. 3, C and F).

Fig. 5 shows relevant controls. No new receptors were visualized in the presence of an excess of BTX (Fig. 5 A). In the absence of unconjugated BTX, simultaneous labeling with mAb 35 and RBTX produced identical ACHR patterns (Fig. 5 B).

Growth Cone Influences on Mobility

The values employed in our model were derived from measurements on uninnervated areas of myotube membrane. If the receptor mobility is substantially different during the initial stages of cluster formation, our predictions might be altered. The diffusion-trapping mechanism could conceivably operate initially on the first ACHRs entering into a cluster, followed by subsequent directed entry of cytoplasmic receptors. Since growth cone–myotube contacts are a likely place to encounter the initial stages of NARP formation (Role et al., 1987; Cohen et al., 1987; Dubinsky et al., 1988), we examined the mobility of ACHRs around advancing and stationary (no net movement over 30 min) growth cones on myotubes after 15 h of coculture.

We examined 47 diffusely labeled spots around the tips of 14 different growth cones. The diffusion coefficient for eight spots within 10 μm of a growth cone was (1.1 $\pm$ 0.3) $\times$ 10^{-9} cm^2/s. For eight paired spots further away on the same muscles, $D = (4.4 \pm 0.7) \times 10^{-10}$ cm^2/s was significantly different (two tailed t test on paired differences $p = 0.027$). Although the diffusion coefficient tended to be faster in front
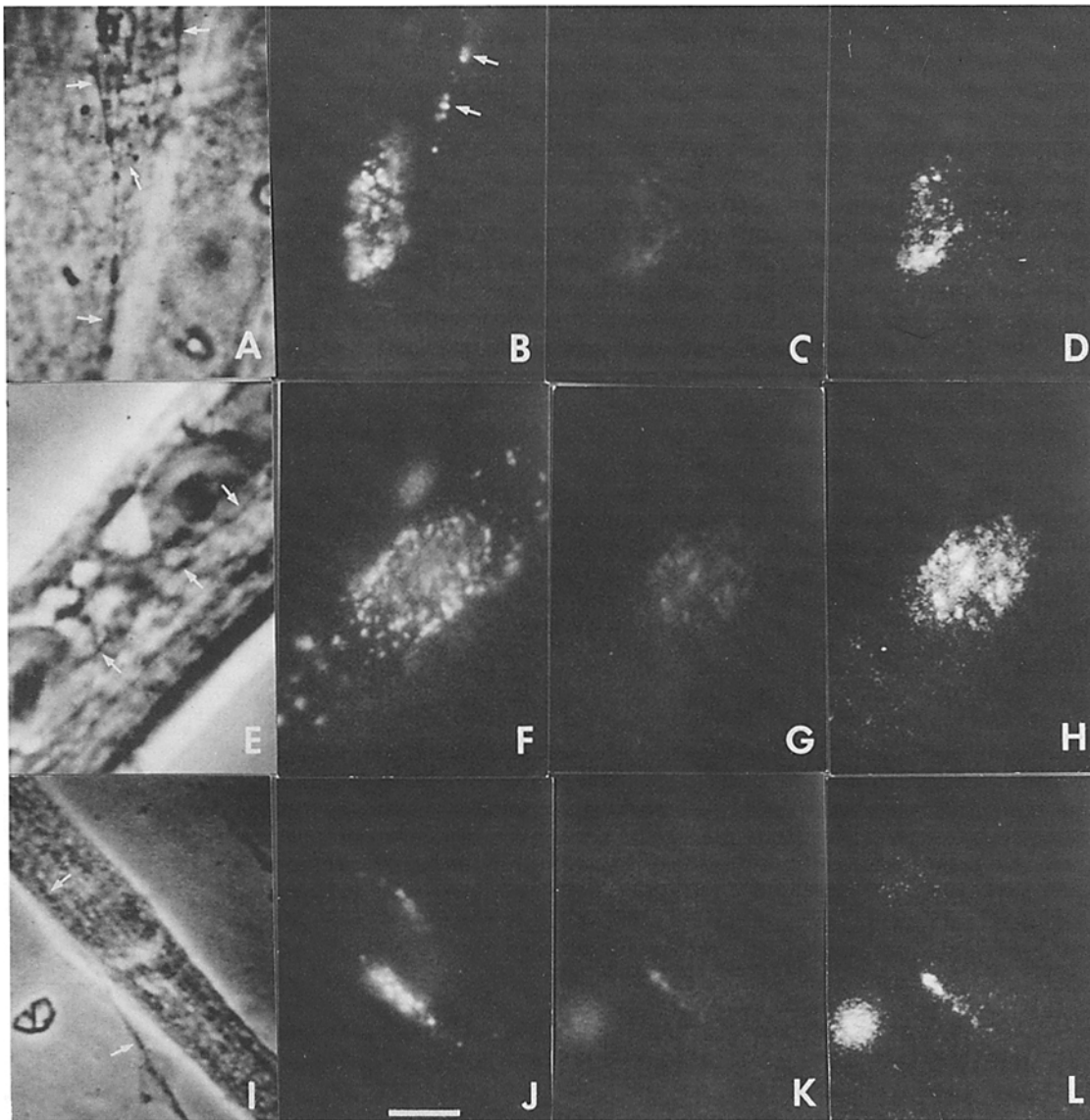
Figure 4. Visualization of newly inserted ACHRs at three different NARPs. *A, E,* and *I* are high power digital phase images of neurites (*arrows*) over myotubes. *B, F,* and *J* are digital fluorescence images of mAB 35 postlabeling of all ACHRs in the NARPs. *C, G,* and *K* contain images of 1 h of newly inserted ACHRs labeled with RBTX. All pixels with intensities above background in *C, G,* and *K* are digitally enhanced in *D, H,* and *L* for easier visualization of those areas where newly inserted receptors occur. Arrows indicate NARPs without any newly inserted receptors. Compare *D* and *H* with the model results computed for the same NARPs in Fig. 3, *C* and *F,* respectively. Bar, 10 μm.

of stationary growth cones, no statistically significant differences were detected between moving and stationary growth cones, $(1.2 \pm 0.4) \times 10^{-9}$ cm^2/s; $N = 4$ vs. $(7.32 \pm 1.9) \times 10^{-10}$ cm^2/s; $N = 6$, $p = 0.29$. Within 10 μm of the growth cone tip 45% $\pm$ 4% (N = 20) of ACHRs diffused in the fast phase, statistically equivalent to 39% $\pm$ 4% ($N = 27$) of ACHRs further away. Although this increased rate of diffusion may enhance accumulation of locally mobile receptors, a twofold increase in the diffusion coefficient would not appreciably alter the behavior observed in the diffusion-trapping model.

Although all growth cones were cholinergic, we do not know if they were involved in the process of synapse formation at the time examined. With this in mind, it is worth mentioning that in three instances, a large decrease in the fractional mobility within 10 μm of a growth cone was observed.

Factors Differentially Affect ACHR Insertion and Mobility

Factors and extracts of chick brain and Torpedo electric organ have been suggested to be involved in receptor accumulation at developing neuromuscular junctions. Therefore, partially purified CBE and TEOE were tested for their ability to modulate ACHR mobility as measured by FPR. CBE increases the rate of insertion of ACHRs (Jessell et al., 1979; Usdin et al., 1986), whereas TEOE increases the overall number of receptor patches.
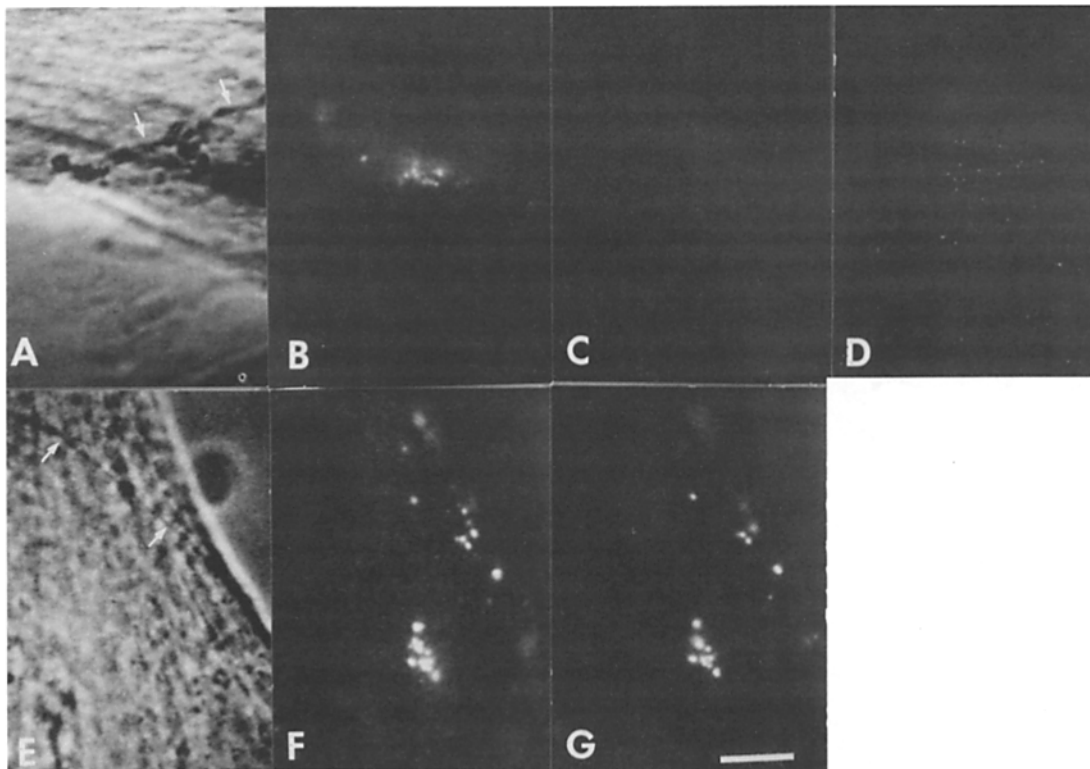
Figure 5. Control experiments. First row (*A-D*) illustrates absence of RBTX label (1 h incubation) in the continued presence of excess unconjugated BTX. Second row (*E-G*) illustrates equivalence of mAb 35 and RBTX label in the absence of any BTX preincubation. *A* and *E* are high power digital phase images of neurites (*arrows*) over myotubes. *B* and *F* are digital fluorescence images of mAb 35 postlabeling of all ACHRs in these NARPs. *C* and *G* contain digital images of 1 h of RBTX-labeled ACHRs. All pixels with the highest intensities in *C* are digitally enhanced in *D* for easier visualization of those areas where any specific RBTX label might occur. Note the scattered positions of these pixels do not correspond to the area of mAb 35 label in *B*. Bar, 10 μm.

Photometer measurements of fluorescence intensity before photobleaching were used as measures of ACHR density (Table III). Ratios of intensities of factor treated cultures compared to controls are presented in Fig. 6 *A*. As expected from ^{125}I-BTX measurements, in TEOE-treated cultures, intensities of diffusely distributed and aggregated ACHRs were identical to controls (Godfrey et al., 1984). Also as expected, CBE-treated cultures increased the overall density of ACHRs (Jessell et al., 1979; Buc Caron et al., 1983; Usdin et al., 1986). However, in the CBE-treated cultures, the intensity of ACHRs aggregated into hot spots increased an average of 4.7-fold (in three separate experiments) while the density in diffuse areas only increased by a factor of 2.1 (Fig. 6 *A*).

FPR of cultures treated with either extract revealed no change in the fast phase diffusion coefficient of ACHRs in diffuse areas (Fig. 6 *B*). In hot spots, ACHRs remained effectively immobile after both treatments (data not shown). Therefore, it appeared that neither CBE nor TEOE altered the rates at which ACHRs moved in the muscle membrane.

TEOE, but not CBE, markedly reduced the fraction of ACHRs that moved in the fast phase. This fractional mobility was measured from the proportion of fluorescence that recovered at 75 s (Fig. 6 *C*). A similar reduction was observed when total recovery was estimated from curves fitted to FPR traces.

Discussion

We have demonstrated that in chick myotubes, new ACHRs are inserted directly into receptor clusters induced by nerve processes. Calculations based on measured diffusion coefficients of mobile ACHRs indicate that a trapping mechanism would lead to a different distribution of receptors than the one that was actually observed.

Diffusion of Nonclustered ACHRs

Unlike other membrane proteins, we have found that FPR estimates of ACHR diffusion coefficient do not scale with the w^2 of different objective lenses as expected for simple diffusion. Our results suggested that the limiting process for fluorescent recovery with the highest power objective was no longer diffusion but rather some other process that was independent of spatial scale (cf., Elson and Reidler, 1979). This constraint could result from interaction of the ACHR with immobile structures in the membrane or underlying cytoskeleton. Previous observation of objective size–dependent diffusion coefficients has been interpreted to result from micron-scale differences in membrane protein composition (Yechiel and Edidin, 1987). Even the faster moving class of ACHRs had a diffusion coefficient that is approximately an order of magnitude lower than expected for simple diffusion limited only by the viscosity of the membrane lipid bilayer
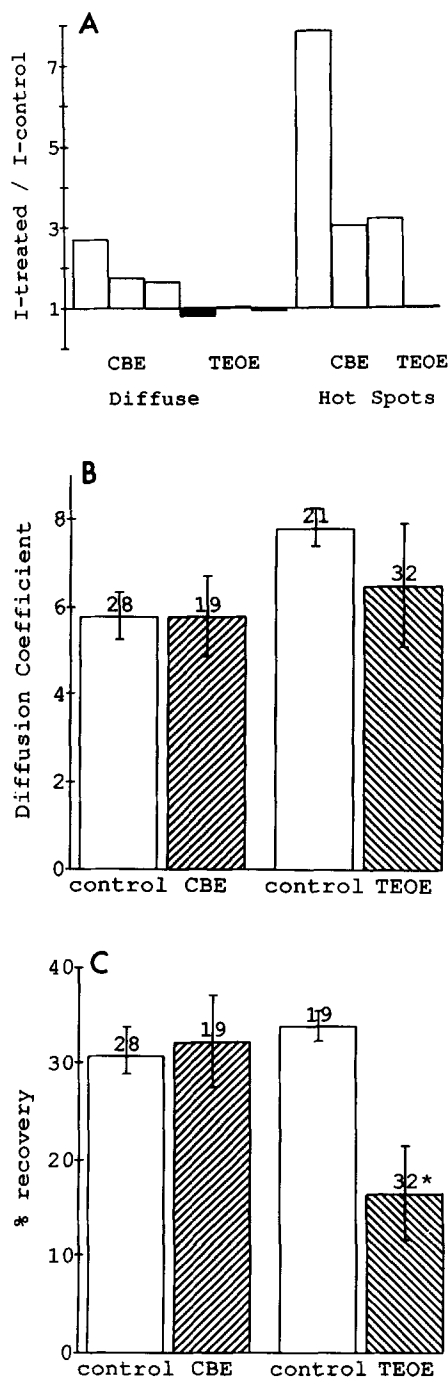
Figure 6. Effects of CBE and TEOE on FPR measurements. (A) Ratios of prebleach intensities (photometer counts) for treated and control cultures increase with CBE treatment but not with TEOE. Raw data from Table III. Open bars represent CBE experiments. Filled bars are TEOE experiments. (B) Fast phase diffusion coefficients were measured from indicated number of bleaches for all factor experiments. Open bars are control sister cultures. Right hatches indicate CBE-treated cultures. Left hatches indicate TEOE treated cultures. (C) Percent of ACHRs in the fast phase. Percent mobility is measured from the amount of fluorescence that recovers at 75 s after the bleach. Bars as in B.

(Schlessinger et al., 1976; Tank et al., 1982). The structural basis of this retardation which has been observed with other membrane proteins is not well understood despite elegant attempts to characterize the responsible interactions (Edidin and Zunigo, 1986; Livneh et al., 1986; Scullion et al., 1987).

As an example of how time dependent receptor interactions could cause the dependence on w, we consider the possibility that the mobile receptors bind reversibly to immobile structures in the membrane. A similar argument could be constructed for a model in which receptor diffusion was constrained by filament matrix cages (Koppel et al., 1981). We would expect that the rate of forming the retarding interactions R_f should be proportional to the concentrations of unbound ACHR C_R and unoccupied interaction sites C_S. Then, $R_f = k_f C_R C_S$. Similarly, the rate of breaking the interactions R_b should be proportional to the concentration of bound sites C_B: $R_b = k_b C_B$. Both R_b and R_f are independent of w. The characteristic chemical relaxation time of the interaction would be $t_c = [k_f \overline{C_R} \overline{C_S} + k_b]^{-1}$, where $\overline{C_R}$ and $\overline{C_S}$ are the steady-state concentrations of the free ACHR and unoccupied sites.

Whether or not FPR measurements will scale as simple diffusion depends on the relative magnitudes of t_c and the characteristic diffusion time, $t_D = w^2/4D$ (Elson and Reidler, 1979). If $t_D > t_c$ then the receptor could experience many interactions during the migration of unbleached fluorophores into a bleached area and thereby seem to be executing simple diffusion at a rate determined by the fraction of time the receptor was unbound and the diffusion coefficient of the unbound receptor. If, however, for smaller values of w, $t_c > t_D$ then the fluorescence recovery rate would be limited by the kinetics of the interaction rather than the rate of diffusion and therefore the dependence on w would weaken, as we have observed. This reasoning leads to the conclusion that t_c, which is proportional to the lifetime of the constraining interaction, must be larger than the value of $t_D = 2.7$ s expected for the 100× objective and may be in the range of the measured recovery time of 13.2 s. If t_D were sufficiently small, it should be possible to observe that the previously uniformly mobile ACHRs would divide into two classes: one, consisting of ACHRs bound throughout the recovery period, which was immobile on the time scale of unimpeded diffusional recovery (i.e., t_D) and the other, the unbound ACHR, diffusing at a rate unimpeded by interactions. On a longer time scale in the range of t_c, the recovery of the apparently immobile fraction would appear to be independent of w. Unfortunately, it is difficult to reduce w to a value smaller than that obtained with the 100× objective, which is already close to the diffraction limit.

A second unexpected property of ACHR diffusion that we have observed was the presence of a subset of ACHRs that diffused at intermediate rates (20-fold more slowly than the most rapidly diffusing subset). It is possible that the apparently immobile fraction of other membrane proteins may also include a fraction of slowly moving molecules. The structural and mechanistic explanation of the slow phase is unclear. Both the dynamic cage model and the reversible anchorage model could be extended to account for the slowly diffusing receptors. A second class of cages or reversible anchorage sites could exist with characterisitic recovery or relaxation times of ~300 s. ACHR-associated proteins present on the cytoplasmic surface of myotube membrane have

Table III. Prebleach Photometer Counts, Mean ± SEM (N)

Experiment	Diffuse		Hotspots	
	Control	CBE	Control	CBE
814	409 ± 111 (6)	1,121 ± 167 (8)‡	1,499 ± 333 (8)	11,744 ± 3,098 (6)*
821	511 ± 70 (16)	908 ± 132 (6)‡	2,050 ± 490 (8)	6,250 ± 2,244 (4)
615	286 ± 43 (6)	481 ± 74 (5)*	2,267 ± 929 (5)	7,303 ± 966 (5)‡
	Control	TEOE	Control	TEOE
612	1,047 ± 256 (5)	836 ± 84 (13)	5,635 ± 1,993 (5)	5,838 ± 1,686 (5)
817	404 ± 28 (10)	421 ± 40 (13)		
924	333 ± 56 (7)	308 ± 51 (6)		

* $p < 0.04$
‡ $p < 0.01$

been implicated in receptor immobilization within clusters (Froehner et al., 1981; Froehner, 1988; Bloch and Morrow, 1989; Carr, C., S. D. Cohen, and G. D. Fischbach, unpublished observations). If these peripheral proteins are associated with diffusely distributed receptors, they might function as reversible binding sites or might contribute to dynamic cage formation. Their precise role in regulating the different phases of mobility described here remains to be determined.

Formation of aggregates of ACHR molecules due to self association might also influence the measured rate of diffusion. Arguing against this suggestion is the demonstration that no immobile or slowly moving fraction is seen in FPR measurements of ACHR mobility on myotube blebs, for which self-association should still be possible (Tank et al., 1982). Furthermore, to account for the slowly mobile fraction aggregates containing ∼1,000 receptors with diameters near 0.6 μm would be required (cf., Saffman and Delbruck, 1977). Although application of the Saffman-Delbruck theory to such large aggregates may overestimate the required aggregate size, even substantially smaller aggregates should be directly detectable by fluorescence microscopy. Indeed, minute fluorescence speckles are often seen among RBTX-labeled, diffusely distributed ACHRs. Whether the particles in these speckles diffuse more slowly than ACHR monomers remains to be determined.

Mechanism of Acetylcholine Receptor Accumulation

As previously reported in studies of other species (Stya and Axelrod, 1983; Kuromi et al., 1985; Stollberg and Fraser, 1988), we find that lateral diffusion of ACHRs on chick myotube membranes is consistent with a diffusion-trapping mechanism of receptor accumulation. Diffusely distributed receptors moving at the fastest rate we have measured, would travel a root mean square distance of ∼30 μm in 1 h, which is sufficient to account for the formation of a 3-μm-diam receptor cluster of two to three times the nearby receptor density within 3 h. However, comparison of direct observations of newly inserted receptor molecules with the prediction of a diffusional model (Figs. 3 and 4) implies that receptor migration plays a minor role in the early stages of NARP formation on chick myotubes. Increasing the diffusional rate within a patch would allow a more rapid redistribution of receptors, similar to the observed experimental result. Hence our conclusion depends upon the experimentally measured upper bound for diffusion of clustered receptors.

A control system may exist that directs newly inserted receptors to specific sites on the surface. Indeed, coated vesicles containing ACHRs, observed by EM enroute to the surface near hot spots (Bursztajn and Fischbach, 1984) and adjacent to receptor clusters (Cohen and Pumplin, 1979), contribute to the increased rate of ACHR insertion at clusters (Bursztajn et al., 1985). ACHRs have been detected in a population of coated vesicles from myotubes by density gradient centrifugation techniques (Porter-Jordan et al., 1986). Fine filamentous structures have also been observed beneath neuromuscular junctions in electronmicrographs from chick and rat myotubes (Burrage and Lentz, 1981; Olek et al., 1986). Newly inserted receptors have been shown to contribute to hot spot formation in rat myotubes (Stya and Axelrod, 1983), but comparable experiments to examine insertion of ACHR have not been performed in Xenopus myocyte cultures.

The distinct borders around receptor clusters imply that some anchoring mechanism restricts all receptors, new and old, within the cluster. Therefore, even with a directed insertion mechanism, an anchoring or "trapping" mechanism is required.

Factors purified from CBE increase the overall rate of receptor insertion in chick myotube membranes (Jessell et al., 1979; Buc-Caron et al., 1983; Usdin and Fischbach, 1986; Harris et al., 1988). Our photometer measurements were sensitive enough to detect this increase in receptor density at nonclustered areas. In addition, we have found that the increase in receptor density at clusters was 2.3 times greater than the increase in density in nonclustered regions. These measurements are consistent with the increased rate of insertion observed at developing synapses (Role et al., 1985). The greater increase in receptor density at hot spots compared to extra cluster regions in CBE-treated cultures is consistent with the notion that an endogenous factor increases ACHR insertion preferentially at developing synapses. We have noted that the maximum receptor density within NARPs is not greater than the density at hot spots in control, untreated myotubes. Therefore, while the nerve may influence the rate of cluster formation, the postsynaptic myotube appears to determine the final receptor concentration (Dubinsky et al., 1988).

Since receptor clusters are more frequently associated with growth cones than other regions of neurites (Role et al., 1987; Cohen et al., 1987; Dubinsky et al., 1988), it is interesting that the rate of ACHR diffusion appeared to be en-

hanced in the vicinity of growth cone–myotube contacts. The faster diffusion did not alter the predictions of our model, but the phenomenon is of interest. It may reflect changes in other cytoskeletal or basement membrane components necessary for assembly of the forming receptor patch, perhaps brought about by molecules or proteases secreted from growth cones (Pittman, 1985; Patterson, 1988). Alternatively, it has been suggested that growth cones may be the source of local electric fields that enhance and direct receptor movement into clusters (Stollberg and Fraser, 1988).

A partially purified factor from Torpedo electric organ basal lamina restricted the mobility of a portion of the diffusely distributed ACHRs but did not alter the diffusion coefficients of the remaining mobile receptors. Media conditioned by a neuroblastoma–glioma hybrid cell line similarly limits the number of receptors that are free to move in rat myotube membranes (Axelrod et al., 1981). These data support the hypothesis that TEOE may be involved in anchoring the receptor (Nitkin et al., 1987; Reist et al., 1987). Antibodies directed against AGRIN, a protein purified from TEOE, are present in the synaptic cleft of regenerating adult neuromuscular junctions and in the myotome of developing limbs (Reist et al., 1987), so it may be present in developing synapses as well. The exact time of appearance of AGRIN during formation of receptor clusters is yet to be determined.

In sum, the accumulation of receptors at developing synapses is complex. The observed distribution of newly inserted receptors throughout large NARPs can not be explained by the diffusion and trapping mechanism. This supports the assertion that in chick myotubes, the directed insertion of ACHRs contributes substantially to development of postsynaptic sites.

References

Andersen, M. J., and M. W. Cohen. 1977. Nerve-induced and spontaneous redistribution of acetylcholine receptors on cultured muscle cells. *J. Physiol. (Lond.).* 268:757–773.

Axelrod, D., P. Ravdin, D. E. Koppel, J. Schlessinger, W. W. Webb, E. L. Elson, and T. R. Podleski. 1976. Lateral motion of fluorescently labeled acetylcholine receptors in membranes of developing muscle fibers. *Proc. Natl. Acad. Sci. USA.* 73:4594–4598.

Axelrod, D., A. Wight, W. Webb, and A. Horwitz. 1978. Influence of membrane lipids on acetylcholine receptor and lipid probe diffusion in cultured myotube membrane. *Biochemistry.* 17:3604–3609.

Axelrod, D., H. C. Bauer, M. Stya, and C. N. Christian. 1981. A factor from neurons induces partial immobilization of nonclustered acetylcholine receptors on cultured muscle cells. *J. Cell Biol.* 88:459–462.

Bloch, R. J., and J. S. Morrow. 1989. An unusual β-spectrin associated with clustered acetylcholine receptors. *J. Cell Biol.* 108:481–493.

Buc-Caron, M. H., P. Nystrom, and G. D. Fischbach. 1983. Induction of acetylcholine receptor synthesis and aggregation. Partial purification of low molecular weight activity. *Dev. Biol.* 95:378–386.

Burrage, T. G., and T. L. Lentz. 1981. Ultrastructural characterization of surface specializations containing high-density acetylcholine receptors on embryonic chick myotubes in vivo and in vitro. *Dev. Biol.* 85:267–286.

Bursztajn, S., and G. D. Fischbach. 1984. Evidence that coated vesicles transport acetylcholine receptors to the surface membrane of chick myotubes. *J. Cell Biol.* 98:507–517.

Bursztajn, S., S. A. Berman, J. L. McManaman, and M. L. Watson. 1985. Insertion and internalization of acetylcholine receptors at clustered and diffuse

domains on cultured myotubes. *J. Cell Biol.* 101:104–111.

Cohen, S. A., and D. W. Pumplin. 1979. Clusters of intramembrane particles associated with binding sites for α-bungarotoxin in cultured chick myotubes. *J. Cell Biol.* 82:494–516.

Cohen, M. W., E. Rodrieguez-Marin, and E. M. Wilson. 1987. Distribution of synaptic specializations along isolated motor units formed in Xenopus nerve-muscle cultures. *J. Neurosci.* 7:2849–2861.

Devreotes, P. N., J. M. Gardner, and D. M. Fambrough. 1977. Kinetics of biosynthesis of acetylcholine receptor and subsequent incorporation into plasma membrane of cultured chick skeletal muscle. *Cell.* 10:365–373.

Dubinsky, J. M., M. Morgan, and G. D. Fischbach. 1988. Variation among acetylcholine receptor clusters induced by ciliary ganglion neurons in vitro. *Dev. Biol.* 130:209–219.

Edidin, M., and M. Zuniga. 1984. Lateral diffusion of wild type and mutant L^d antigens in L cells. *J. Cell Biol.* 99:2333–2335.

Edwards, C., and H. L. Frisch. 1976. A model for the localization of acetylcholine receptors at the muscle endplate. *J. Neurobiol.* 7:377–381.

Elson, E. L., and J. A. Reidler. 1979. Analysis of cell surface interactions by measurements of lateral mobility. *J. Supramol. Struct.* 12:481–489.

Fischbach, G. D. 1972. Synapse formation between dissociated nerve and muscle cells in low density cell culture. *Dev. Biol.* 28:407–429.

Frank, E., and G. D. Fischbach. 1979. Early events in neuromuscular junction formation in vitro. *J. Cell Biol.* 83:143–158.

Froehner, S. C. 1988. The role of the postsynaptic cytoskeleton in ACHR organization. *Trends Neurosci.* 9:37–41.

Froehner, S. C., V. Gulbrandsen, C. Hyman, A. Y. Jeng, R. R. Neubig, and J. B. Cohen. 1981. Immunofluorescence localization at the mammalian neuromuscular junction of the M$_r$ 43,000 protein of Torpedo postsynaptic membranes. *Proc. Natl. Acad. Sci. USA.* 78:5230–5234.

Godfrey, E. W., R. M. Nitkin, B. G. Wallace, L. L. Rubin, and U. J. McMahan. 1984. Components of Torpedo electric organ and muscle that cause aggregation of acetylcholine receptors on cultured muscle cells. *J. Cell Biol.* 99:615–627.

Harris, D. A., D. L. Falls, R. M. Dill-Devor, and G. D. Fischbach. 1988. Acetylcholine receptor-inducing factor from chicken brain increases the level of mRNA encoding the receptor α subunit. *Proc. Natl. Acad. Sci. USA.* 85:1983–1987.

Hirano, H. 1967. Ultrastructural study on the morphogenesis of the neuromuscular junction in the skeletal muscle of the chick. *Z. Zellforsch.* 79:298–208.

James, D. W., and R. L. Tresman. 1969. An electron-microscopic study of the de novo formation of neuromuscular junctions in tissue culture. *Z. Zellforsch. Mikrosk. Anat.* 100:126–140.

Jessell, T. M., R. E. Siegel, and G. D. Fischbach. 1979. Induction of acetylcholine receptors on cultured skeletal muscle by a factor extracted from brain and spinal cord. *Proc. Natl. Acad. Sci. USA.* 76:5397–5401.

Koppel, D. E., D. Axelrod, J. Schlessinger, E. L. Elson, and W. W. Webb. 1976. Dynamics of fluorescence marker concentration as a probe of mobility. *Biophys. J.* 16:1315–1329.

Koppel, D. E., M. P. Sheetz, and M. Schindler. 1981. Matrix control of protein diffusion in biological membranes. *Proc. Natl. Acad. Sci. USA.* 78:3576–3580.

Kuromi, H., and Y. Kidokoro. 1984. Nerve disperses preexisting acetylcholine receptor clusters prior to induction of receptor accumulation in Xenopus muscle cultures. *Dev. Biol.* 103:53–61.

Kuromi, H., B. Brass, and Y. Kidokoro. 1985. Formation of acetylcholine receptor clusters at neuromuscular junction in Xenopus cultures. *Dev. Biol.* 109:165–176.

Livneh, E., M. Benveniste, R. Prywes, S. Felder, Z. Kam, and J. Schlessinger. 1986. Large deletions in the cytoplasmic kinase domain of the epidermal growth factor receptor do not affect its lateral mobility. *J. Cell Biol.* 103:327–331.

Nishi, R., and D. Berg. 1977. Dissociated ciliary ganglion neurons in vitro: survival and synapse formation. *Proc. Natl. Acad. Sci. USA.* 74:5171–5175.

Nitkin, R. M., M. A. Smith, C. Magill, J. R. Fallon, Y. M. Yao, B. G. Wallace, and U. J. McMahan. 1987. Identification of Agrin, A synaptic organizing protein from Torpedo electric organ. *J. Cell Biol.* 105:2471–2478.

Olek, A. J., A. Ling, and M. P. Daniels. 1986. Development of ultrastructural specializations during the formation of acetylcholine receptor aggregates on cultured myotubes. *J. Neurosci.* 6:487–497.

Patterson, P. H. 1988. On the importance of being inhibited, or saying no to growth cones. *Neuron.* 1:263–267.

Pittman, R. N. 1985. Release of plasminogen activator and a calcium-dependent metalloprotease from cultured sympathetic and sensory neurons. *Dev. Biol.* 110:91–101.

Poo, M. M. 1982. Rapid lateral diffusion of functional ACH receptors in embryonic muscle cell membrane. *Nature (Lond.).* 295:332–334.

Porter-Jordan, K., R. J. J. Benson, P. Buoniconti, and R. E. Fine. 1986. An acetylcholinesterase-mediated density shift technique demonstrates that coated vesicles from chick myotubes may contain both newly synthesized acetylcholinesterase and acetylcholine receptors. *J. Neurosci.* 6:3112–3119.

Ravdin, P., and D. Axelrod. 1977. Fluorescent tetramethyl rhodamine derivatives of alpha-bungarotoxin: preparation, separation and characterization. *Anal. Biochem.* 58:585–592.

Reist, N. E., C. Magill, and U. J. McMahan. 1987. Agrin-like molecules in normal, denervated and damaged skeletal muscle. *J. Cell Biol.* 105:2457–2469.

Role, L. W., V. Matossian, R. J. O'Brien, and G. D. Fischbach. 1985. On the mechanism of acetylcholine receptor accumulation at newly formed synapses on chick myotubes. *J. Neurosci.* 5:2197-2220.

Role, L. W., D. Roufa, and G. D. Fischbach. 1987. The distribution of acetylcholine receptor clusters at sites of transmitter release along chick ciliary ganglion neurite-myotube contacts in culture. *J. Cell Biol.* 104:371-379.

Saffman, P. G., and M. Delbruck. 1975. Brownian motion in biological membranes. *Proc. Natl. Acad. Sci. USA.* 72:3111-3113.

Schlessinger, J., D. E. Koppel, D. Axelrod, K. Jacobson, W. W. Webb, and E. L. Elson. 1976. Lateral transport on cell membranes: mobility of concanavalin A receptors on myoblasts. *Proc. Natl. Acad. Sci. USA.* 73:2409-2413.

Scullion, B. F., Y. Hou, L. Puddington, J. K. Rose, and K. J. Jacobson. 1987. Effects of mutations in three domains of the vesicular stomatitis viral glycoprotein on its lateral diffusion in the plasma membrane. *J. Cell Biol.* 105:69-75.

Stollberg, J., and S. E. Fraser. 1988. Acetylcholine receptors and concanavalin A-binding sites on cultured *Xenopus* muscle cells: electrophoresis, diffusion, and aggregation. *J. Cell Biol.* 107:1397-1408.

Stya, M., and D. Axelrod. 1983. Diffusely distributed acetylcholine receptors can participate in cluster formation on cultured rat myotubes. *Proc. Natl. Acad. Sci. USA.* 80:449-453.

Stya, M., and D. Axelrod. 1984. Mobility of extrajunctional acetylcholine receptors on denervated adult muscle fibers. *J. Neurosci.* 4:70-74.

Tank, D. W., E. S. Wu, and W. W. Webb. 1982. Enhanced molecular diffusibility in muscle membrane blebs: release of lateral constraints. *J. Cell Biol.* 92:207-212.

Tzartos, S. J., D. E. Rand, B. L. Einarson, and J. M. Lindstrom. 1981. Mapping of the surface structure of electrophorus acetylcholine receptor using monoclonal antibodies. *J. Biol. Chem.* 256:8635-8645.

Usdin, T. B., and G. D. Fischbach. 1986. Purification and characterization of a polypeptide from chick brain that promotes the accumulation of acetylcholine receptors in chick myotubes. *J. Cell Biol.* 103:493-507.

Yechiel, E., and M. Edidin. 1987. Micrometer-scale domains in fibroblast plasma membranes. *J. Cell Biol.* 105:755-760.